CHAPTER IV

RESULTS AND DISCUSSION

4.1 Characterization of Ni-implanted boron-doped diamond electrode and as-deposited boron-doped diamond electrode

4.1.1 Digital microscope

Optical microscope images of the Ni-implanted diamond electrode and as-deposited diamond electrode were taken using a digital microscope. These images are shown in Figure 4.2 and 4.3, respectively. From these figures, it can be seen that the silicon wafer was fully covered by diamond crystals. The diamond crystal sizes were 5-8 μm. Although no changes in the surface morphology or color were observed an optical microscope image of the surface after the implantation indicates the presence of small holes.

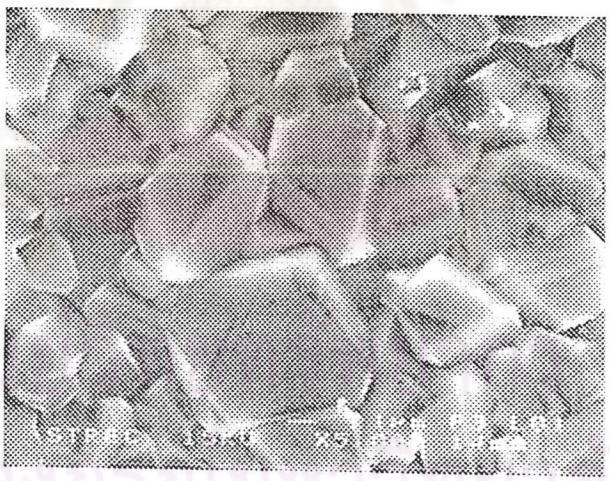

Figure 4.1 Optical microscope image of Ni-implanted diamond electrode

Figure 4.2 Optical microscope image of as-deposited diamond electrode

4.1.2 Raman spectroscopy

Raman measurements were carried out using a Renishaw 2000 System with Ar^+ laser excitation (514.5 nm). Figure 4.4. are the Raman spectra of (a) as-deposited diamond electrode, (b) Ni-implanted diamond electrode, and (c) annealed Ni-implanted diamond electrode, respectively. The spectrum in Figure 4.4a exhibits a sharp first-order peak (single-phonon scattering) at 1332 cm^{-1}, which provides strong evidence for a well-crystallized diamond. After the implantation, not only the peak at 1332 cm^{-1} but also a peak at ~1500 cm^{-1}, related to sp^2 carbon, were observed (Figure 4.3b).

After 10 min of annealing at 850°C, the scattering intensity of the characteristic peak is comparable to that of the as-deposited diamond electrode (Figure 4.3c). This implies that the strained in the diamond film generated by irradiation has been partially relieved by annealing. Usually, this may be achieved by the recombination of excess interstitials and vacancies.

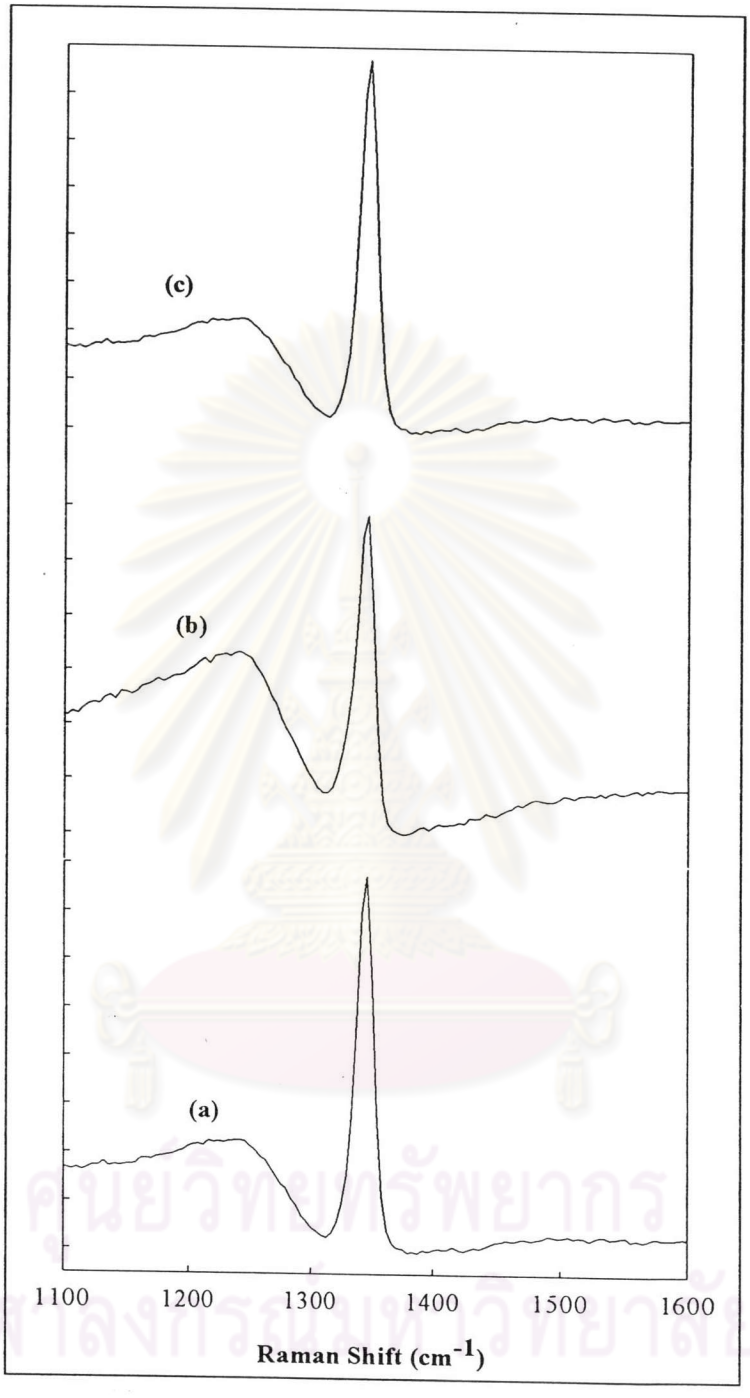

Figure 4.3 Raman spectrum of (a) as-deposited diamond electrode, (b) Ni-implanted diamond electrode and (c) annealed Ni-implanted diamond electrode.

4.2 Cyclic voltammetry

4.2.1 Background current

The preliminary work was focused on a comparison of the background currents that were obtained with the Ni-implanted boron-doped diamond electrode, as-deposited boron-doped diamond electrode and glassy carbon electrode. Figure 4.5, 4.6 and 4.7 show the background voltammograms of 0.1 M phosphate buffer (pH 2) at the Ni-implanted boron-doped diamond electrode, boron-doped diamond electrode and glassy carbon electrode, respectively. The background current for the glassy carbon electrode was appositely 3 times higher than that obtained with the Ni-implanted boron-doped diamond and as-deposited boron-doped diamond electrodes. There are three possibilities that can explain the low background current [6]. First, the relative absence of electroactive carbon-oxygen functionalities on the hydrogen terminated diamond surface as compared with glassy carbon, leads to a lower current but this assumption can only explain only some, but not all, of the low current for diamond. A second contributing factor may be a lower charge carrier concentration due to the semimetal-semiconductor nature of boron-doped diamond. A lower state at given potential, or lower charge carrier concentration, would lead to a reduced accumulation of counterbalancing ions and water dipoles on the solution side of the interface, thereby lowering the background current. A third possible contributing factor could be that the diamond surface is constructed like an array of microelectrodes. In other words, perhaps the diamond surface has "electrochemically active" sites separated by less reactive or more insulating regions, in much the same way that composite electrodes have vary reactive of carbon separated by insulating regions of the support.

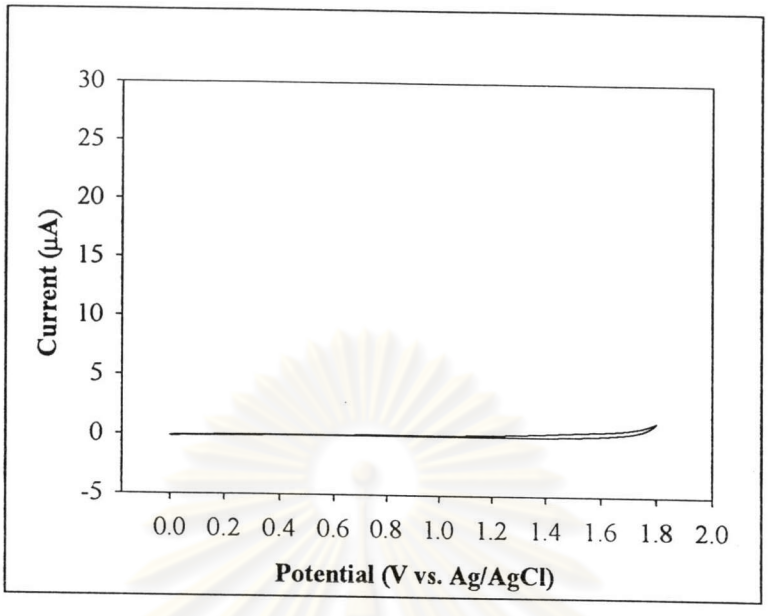

Figure 4.4 Cyclic voltammogram of 0.1 M phosphate buffer (pH 2) at the Ni-implanted boron-doped diamond electrode. The scan rate was 50 mVs^{-1}

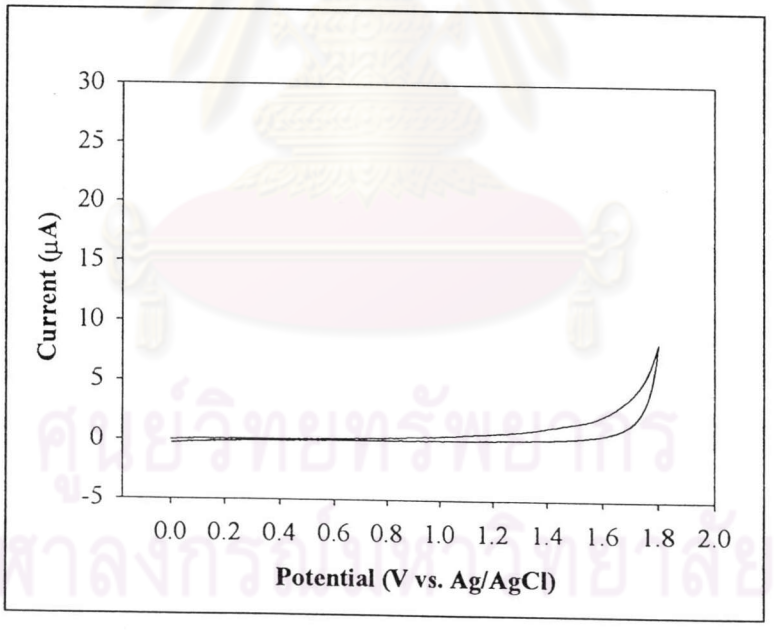

Figure 4.5 Cyclic voltammogram of 0.1 M phosphate buffer (pH 2) at the as-deposited boron-doped diamond electrode. The scan rate was 50 mVs^{-1}

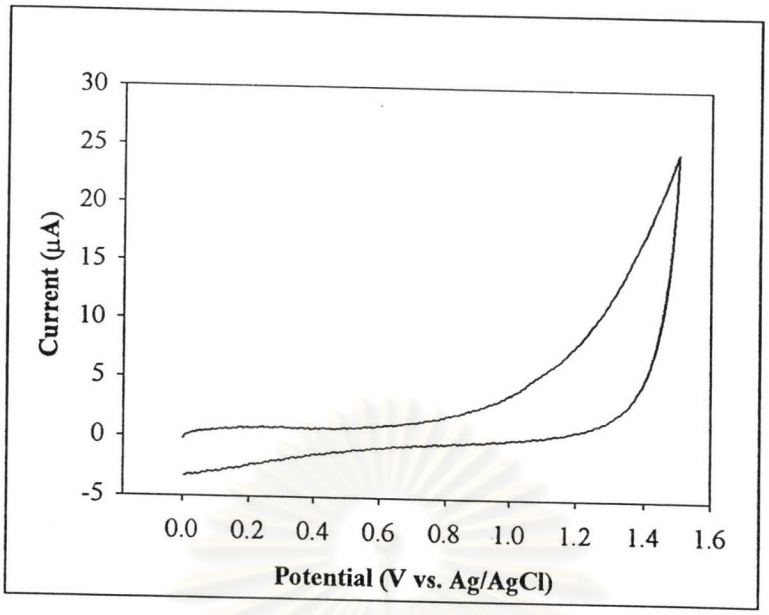

Figure 4.6 Cyclic voltammogram of 0.1 M phosphate buffer (pH 2) at the glassy carbon electrode. The scan rate was 50 mVs^{-1}

4.2.2 pH dependence

Cyclic voltammetry at a Ni-implanted boron-doped diamond electrode was used to study the influence of pH on the electrochemical oxidation of tetracycline hydrochloride. A phosphate buffer was employed as a supporting electrolyte for the amperomatic studies of these antibiotic drugs. The variation of pH from the acidic values to the basic values were regulated by using 0.1 M sodium hydroxide solution or 85 % phosphoric acid. The oxidative voltammetric results of each analyte are discussed below.

4.2.2.1 Tetracycline hydrochloride

Table 4.1 summarizes the electrochemical data obtained from cyclic voltammograms of 1 mM tetracycline hydrochloride oxidation at pH 2, 3, 4, 5, 6, 7, 8, 9, and 10 at the Ni-implanted diamond electrode. The experimental results show that the analyte oxidation peak potential, Ep^{ox} (positive scan) are shifted to more negative values as the pH of the solutions increase. These phenomena may be attributed to the

fact that tetracycline hydrochloride was easier to epimerize to the anhydrotetracycline in acidic media or to isotetracycline in basic media [78]. The proposed mechanisms of the epimerization of this compound are shown in Figure 4.7. In both acidic and alkaline solutions, the epimerization occurred at C-6 hydroxyl group. These occurrences imply that the oxidation process of tetracycline hydrochloride released hydrogen ion into the solution [79], and the reduction process took up hydrogen ion from the solution. From the electrochemical data displayed in Table 4.1, the highest oxidation current response at the oxidation peak potential about 1.516 V vs. Ag/AgCl was obtained at the pH 2. Therefore, this pH value was chosen as the optimum pH for the study of tetracycline hydrochloride. The cyclic voltammograms of tetracycline hydrochloride in different pH solutions are shown in Figure 4.8-4.10, respectively.

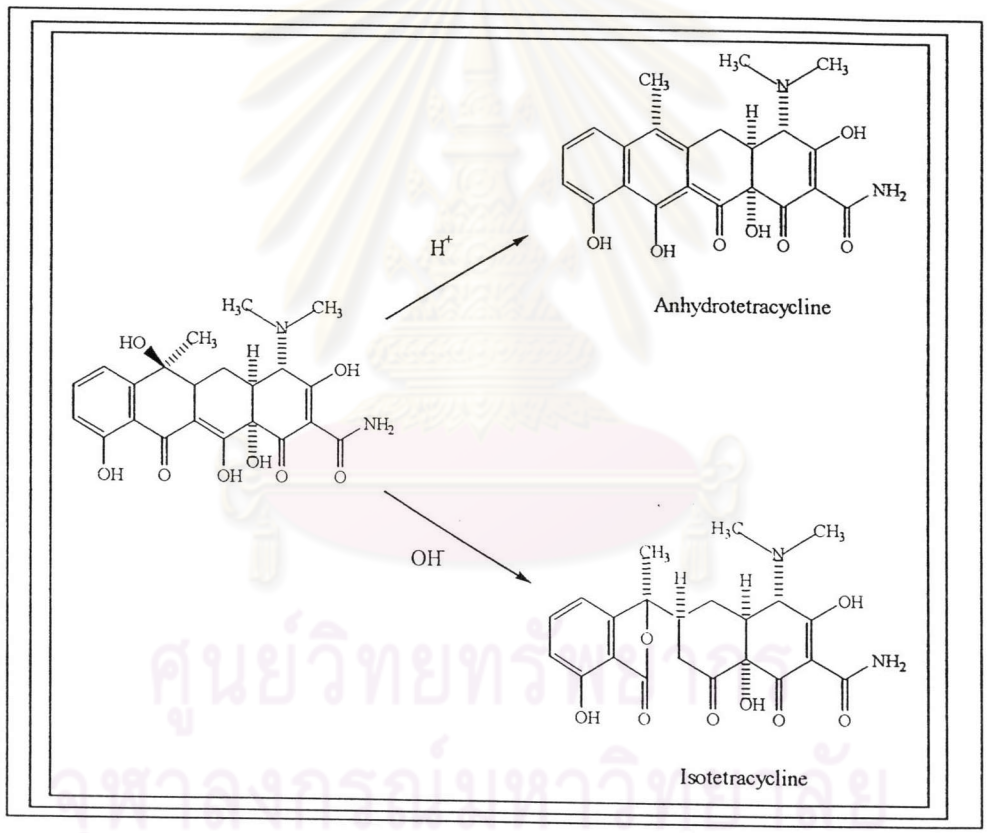

Figure 4.7 The proposed epimerization mechanism of tetracycline [79]

Table 4.1 Comparison of electrochemical data obtained from cyclic voltammograms of the 1 mM tetracycline at pH 2, 3, 4, 5, 6, 7, 8, 9, and 10

pH	E_p^{ox} * (V vs. Ag/AgCl)	I_p^{ox} ** (μA)
2	1.516	34.10
3	1.516	28.90
4	1.506	26.30
5	1.511	26.60
6	1.511	30.40
7	1.511	22.30
8	1.516	22.40
9	1.506	19.00
10	1.486	28.80

* Oxidation peak potential of tetracycline

**Oxidation peak current of tetracycline

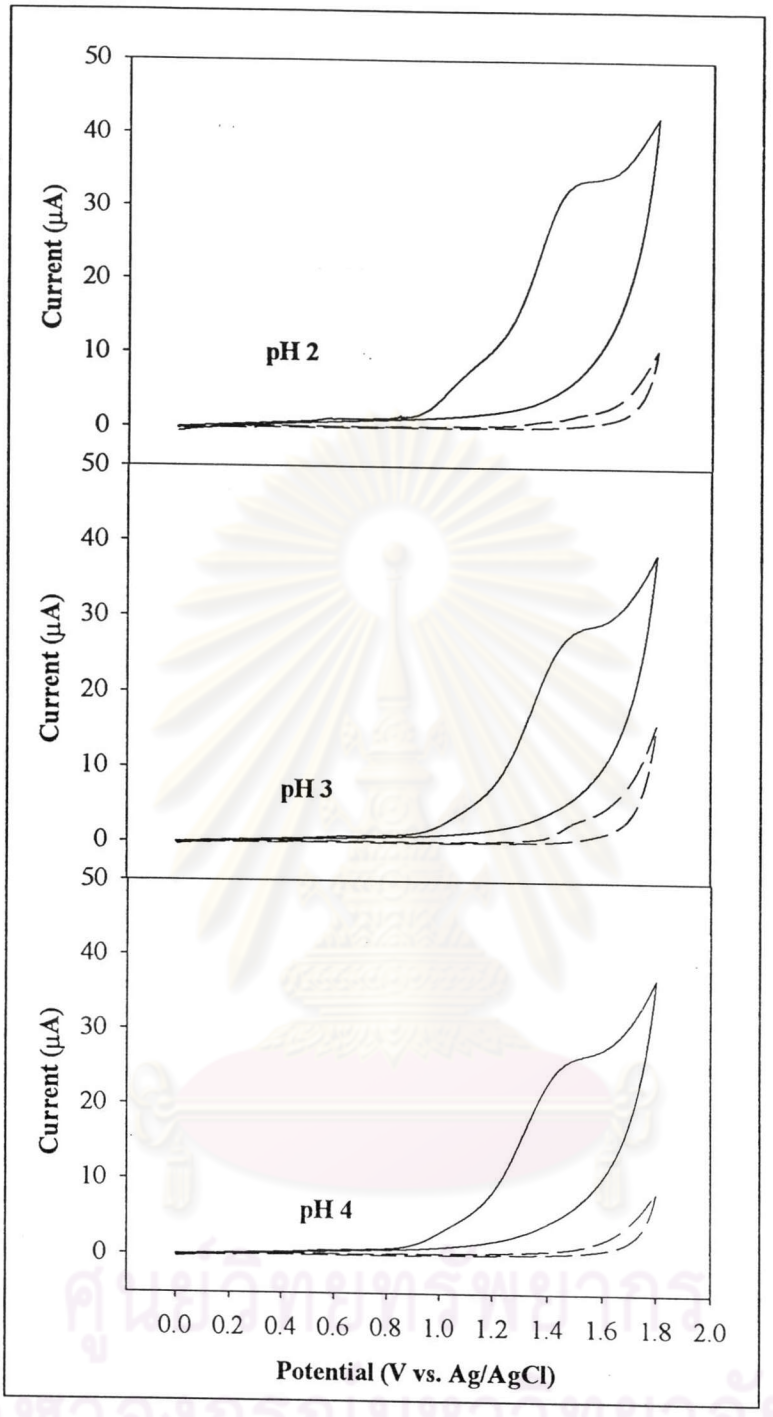

Figure 4.8 Cyclic voltammogram of 1 mM tetracycline in 0.1 M phosphate buffer (pH 2, 3 and 4) at Ni-implanted diamond electrode (solid line). The scan rate was 50 mVs^{-1}. Background voltammogram is also shown in this Figure (dash line).

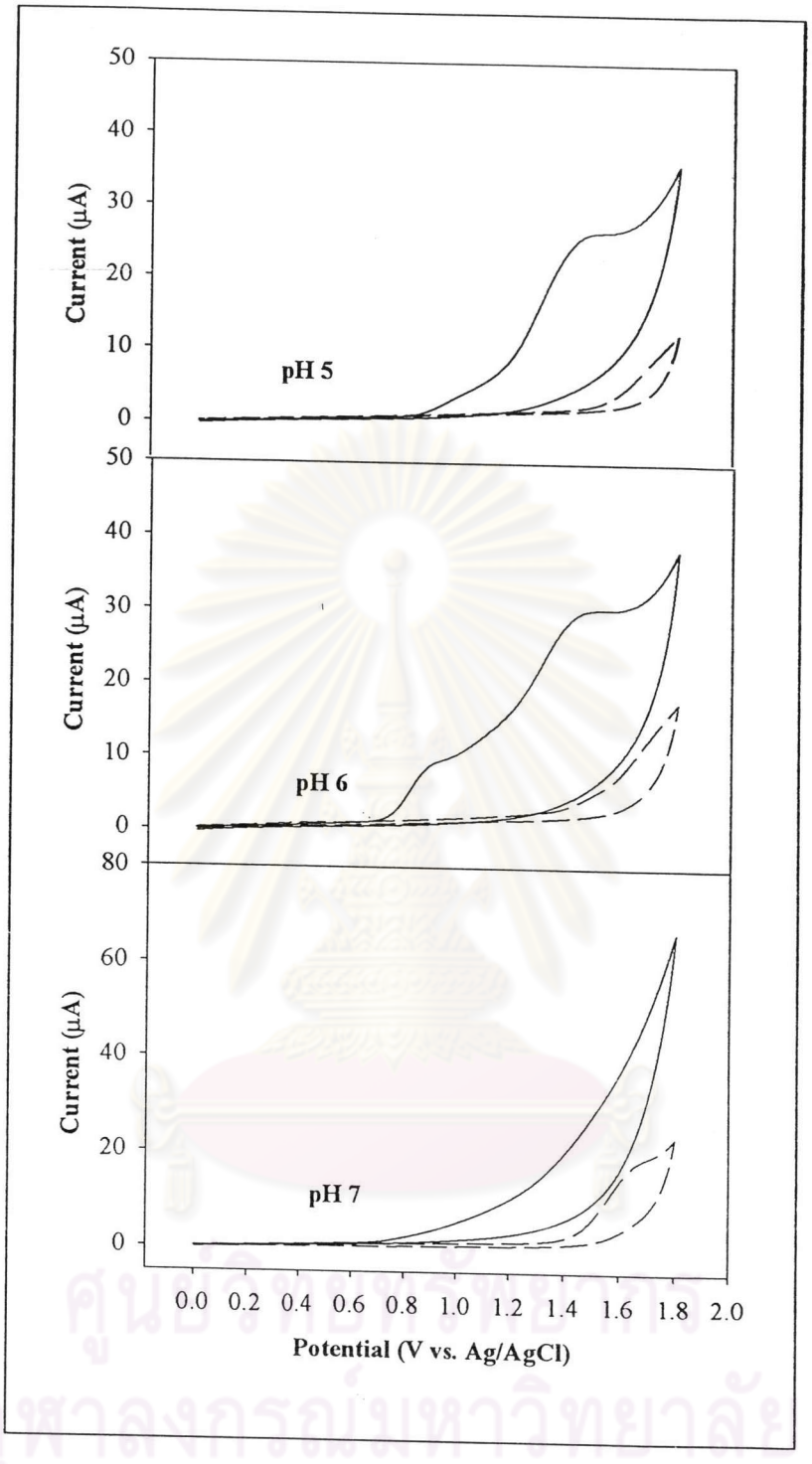

Figure 4.9 Cyclic voltammogram of 1 mM tetracycline in 0.1 M phosphate buffer (pH 5, 6and 7) at Ni-implanted diamond electrode (solid line). The scan rate was 50 mVs^{-1}. Background voltammogram is also shown in this Figure (dash line).

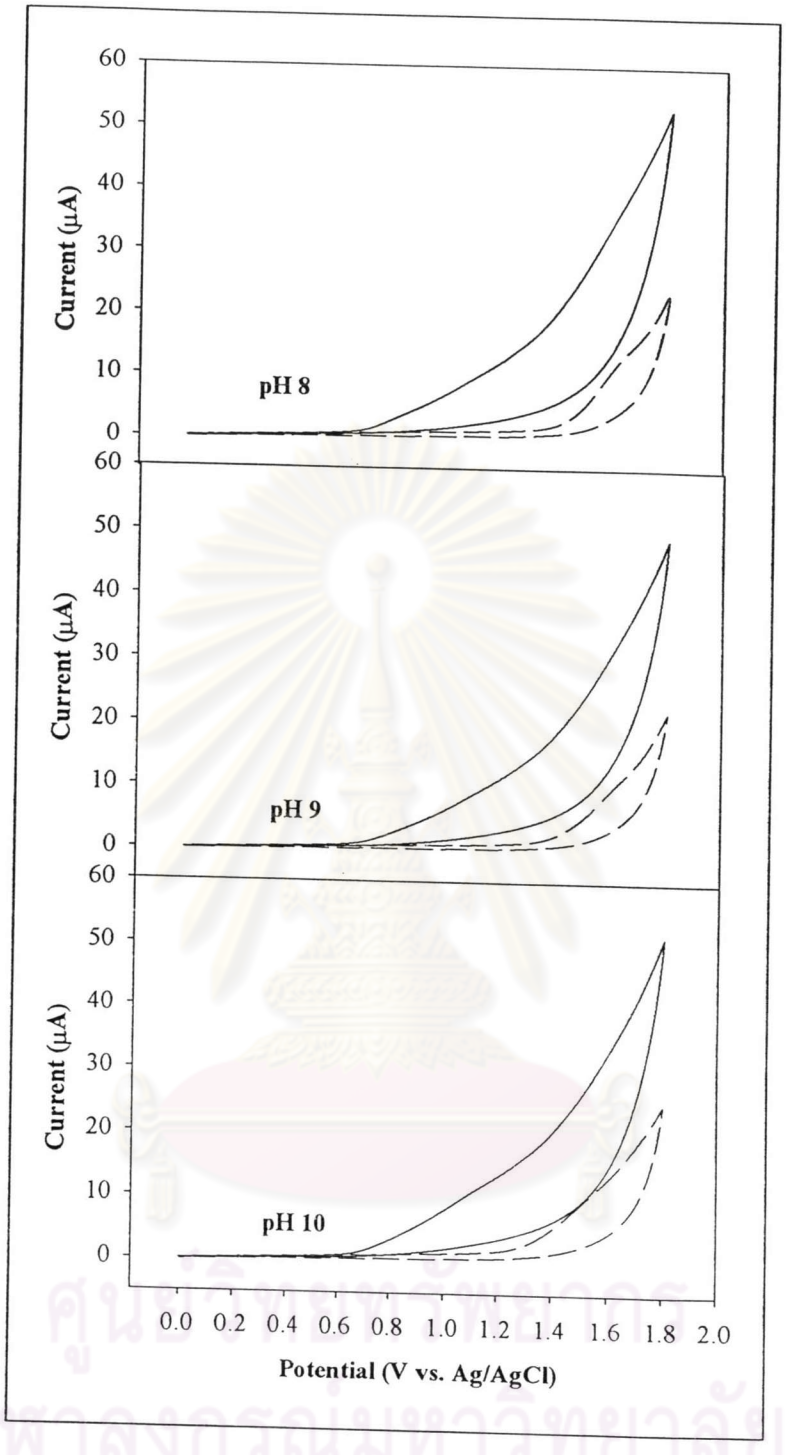

Figure 4.10 Cyclic voltammogram of 1 mM tetracycline in 0.1 M phosphate buffer (pH 8, 9and 10) at Ni-implanted diamond electrode (solid line). The scan rate was 50 mVs^{-1}. Background voltammogram is also shown in this Figure (dash line).

4.2.3 The electrochemical oxidation of the teracyclines

The electrochemical oxidation of 1 mM tetracycline, 1 mM chlortetracycline, 1mM doxycycline and 1 mM oxytetracycline at pH 2 at the Ni-implated diamond electrode, as-deposited diamond electrode and the glassy carbon electrode were studied.

Figure 4.11 show the cyclic voltammograms obtained for 1 mM tetracycline hydrochloride, 1 mM chlortetracycline, 1mM doxycycline and 1 mM oxytetracycline at Ni-implanted diamond electrode, as-deposited diamond electrode and glassy carbon electrode. A well-defined irreversible cyclic voltammograms were obtained at the Ni-implanted diamond electrode and diamond electrode (Figure 4.11a and 4.11b) while an ill-defined irreversible cyclic voltammograms was obtained at the glassy carbon electrode (Figure 4.11c) for all analytes. However, the Ni-inplanted diamond electrode again provided a better S/B ratio current signal. Similar results were also observed with chlortetracycline (Figure 4.12), doxycycline (Figure 4.13) and oxytetracycline (Figure 4.14). The electochemical data obtained from cyclic voltammograms of these solutions at the mentioned electrodes are shown in Table 4.2. It was found that the Ni-implanted diamond electrode provided the highest S/B ratios for tetracycline, chlortetracycline, doxycycline and oxytetracycline among the three electrodes studied.

Table 4.2 The electrochemical data of 1 mM tetracycline, 1 mM chlortetracycline, 1 mM doxycycline and 1 mM oxytetracycline at Ni-implanted diamond electrode, as-deposited diamond electrode and glassy carbon electrode.

Analytes	Electrode	E_p^{ox} * (V)	I_p^{ox} ** (μA)	S/B [a]
Tetracycline	Ni-DIA	1.501	20.90	12.06
	BDD	1.501	17.00	11.56
	GC	1.178	7.10	1.42
Chlortetracycline	Ni-DIA	1.501	17.30	9.61
	BDD	1.438	9.00	6.12
	GC	0.975	7.80	1.56
Doxycycline	Ni-DIA	1.501	16.60	9.22
	BDD	1.477	10.60	7.21
	GC	1.059	7.00	1.40
Oxytetracycline	Ni-DIA	1.511	27.90	15.50
	BDD	1.506	7.80	5.31
	GC	1.064	9.90	1.98

* Oxidation peak potential

**Oxidation peak current

[a] calculated from I_p^{ox}/ background current

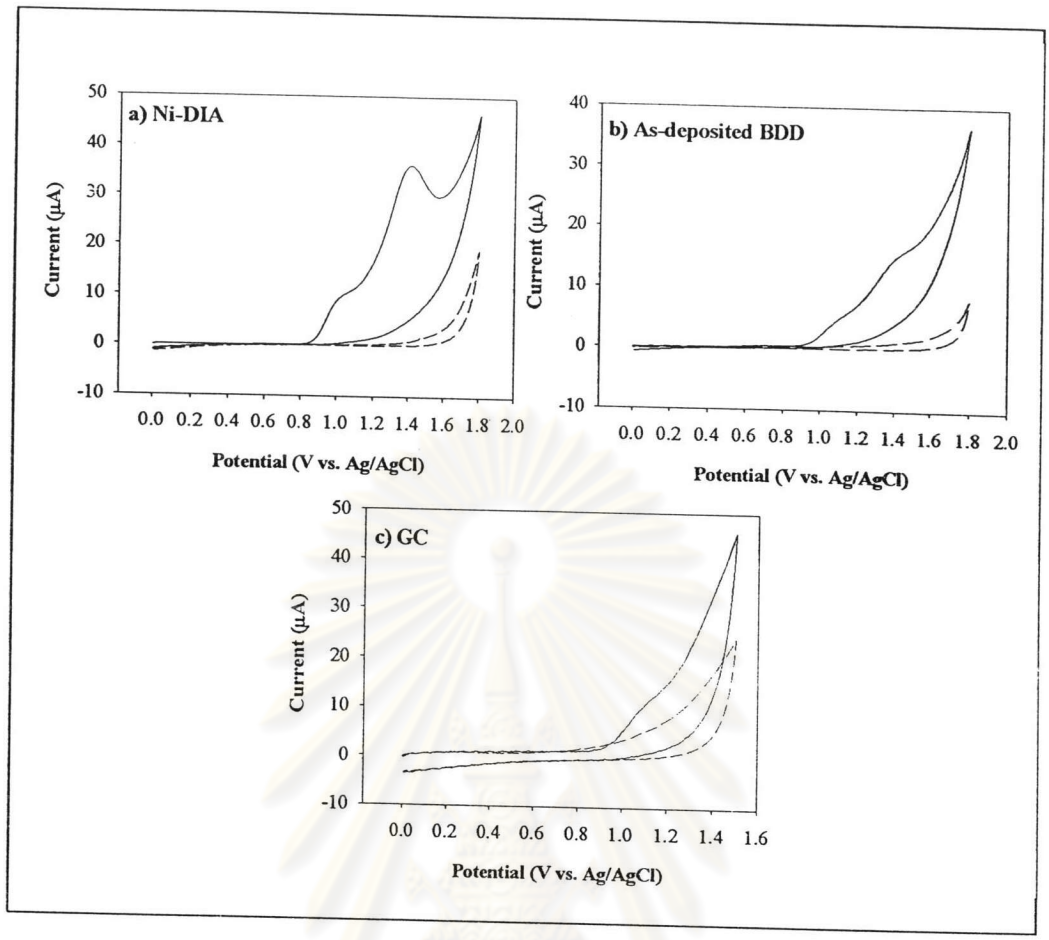

Figure 4.11 Cyclic voltammogram of 1 mM tetracycline in 0.1 M phosphate buffer (pH 2) at Ni-implanted diamond electrode a) As-deposited diamond electrode b) and Glassy carbon c) (solid line). The scan rate was 50 mVs^{-1}. Background voltammogram (0.1 M phosphate buffer, pH 2) is also shown in this Figure (dash line)

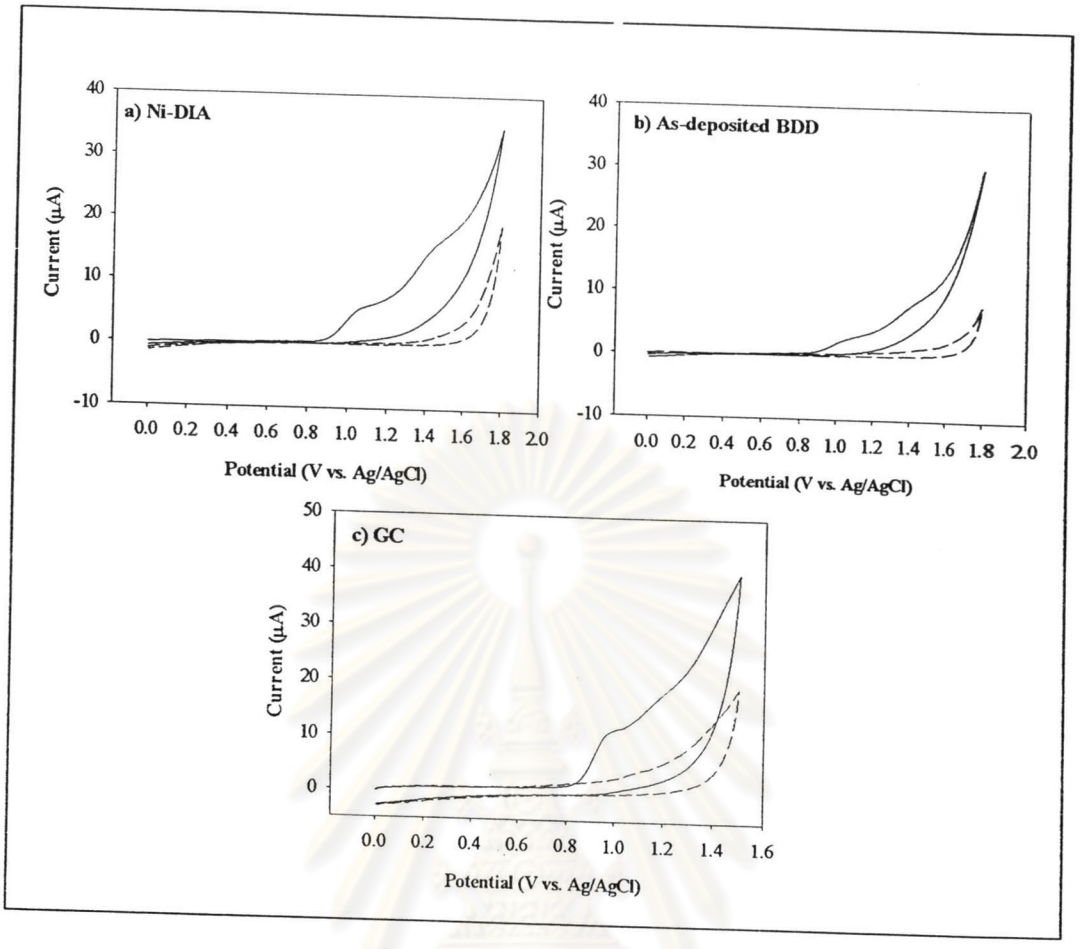

Figure 4.12 Cyclic voltammogram of 1 mM chlortetracycline in 0.1 M phosphate buffer (pH 2) at Ni-implanted diamond electrode a) As-deposited diamond electrode b) and Glassy carbon c) (solid line). The scan rate was 50 mVs^{-1}. Background voltammogram (0.1 M phosphate buffer, pH 2) is also shown in this Figure (dash line)

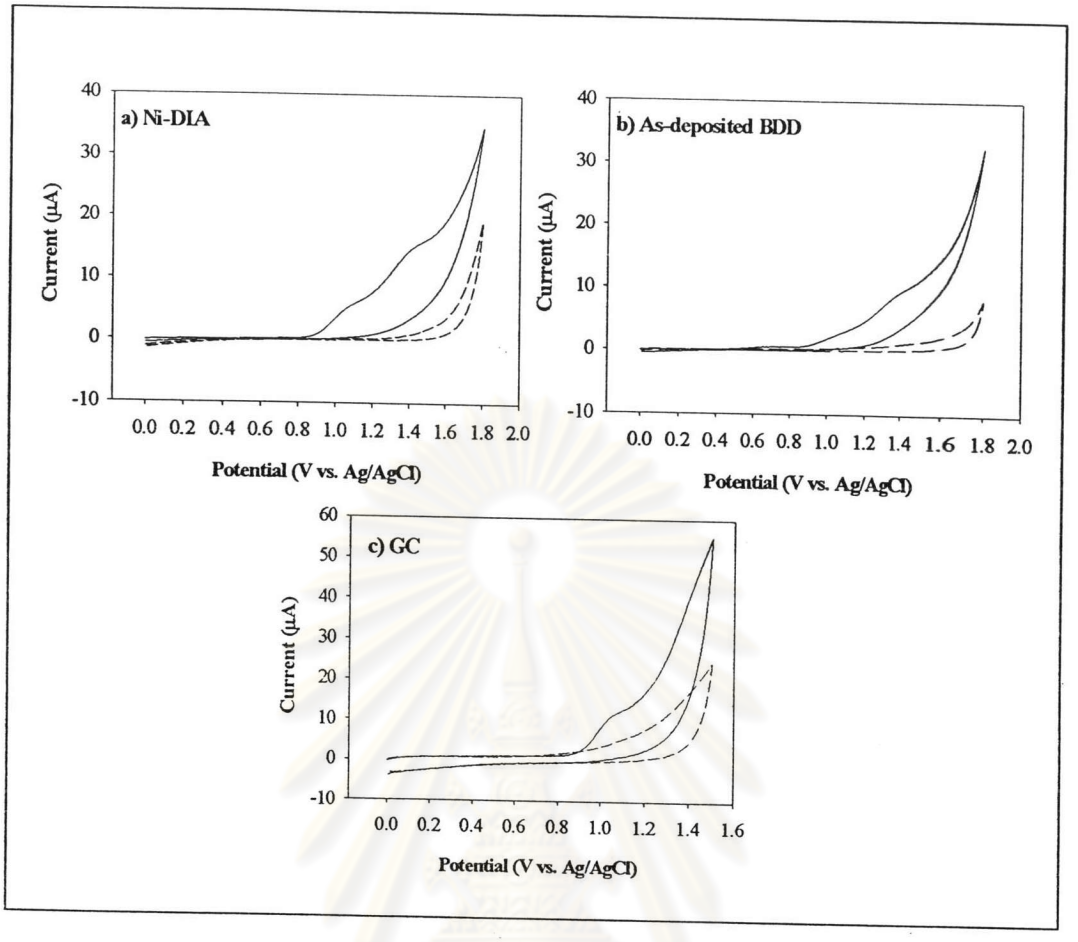

Figure 4.13 Cyclic voltammogram of 1 mM doxycycline in 0.1 M phosphate buffer (pH 2) at Ni-implanted diamond electrode a) As-deposited diamond electrode b) and Glassy carbon c) (solid line). The scan rate was 50 mVs^{-1}. Background voltammogram (0.1 M phosphate buffer, pH 2) is also shown in this Figure (dash line)

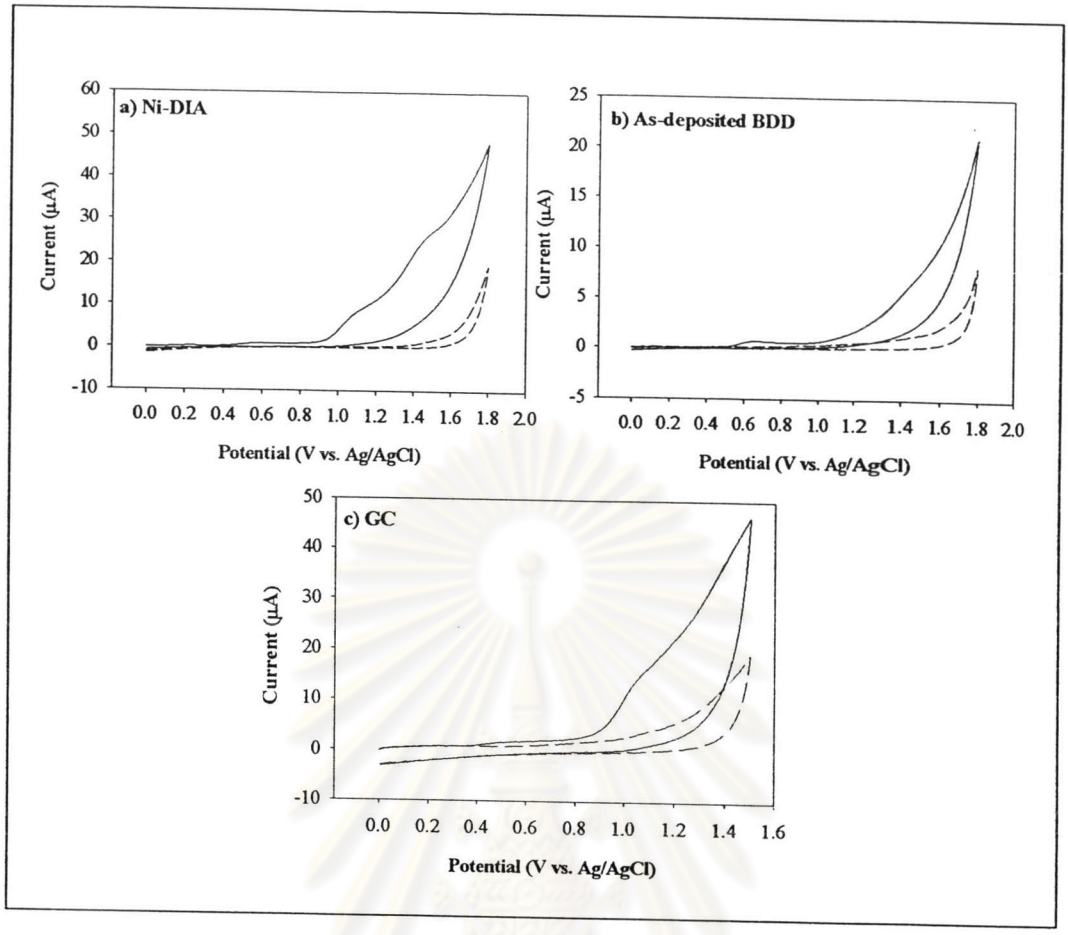

Figure 4.14 Cyclic voltammogram of 1 mM oxytetracycline in 0.1 M phosphate buffer (pH 2) at Ni-implanted diamond electrode a) As-deposited diamond electrode b) and Glassy carbon c) (solid line). The scan rate was 50 mVs^{-1}. Background voltammogram (0.1 M phosphate buffer, pH 2) is also shown in this Figure (dash line)

4.2.4 Effect of scan rate

The effect of the scan rate on the electrochemical behaviors of tetracyclin, chlortetracycline, doxycycline and oxytetracycline was investigated by variation of the scan rate from 10 to 300 mVs^{-1}. Figure 4.15 illustrates the relationship between the current responses and the square root of the scan rate for tetracycline hydrochloride. From these results, the current response of tetracycline hydrochloride was directly proportional to the square root of the scan rate. It can be concluded that the diffusion process control the transportation of these analytes. From the cyclic

voltammograms displayed in these Figures, the oxidation of these selected analytes underwent the irreversible reaction.

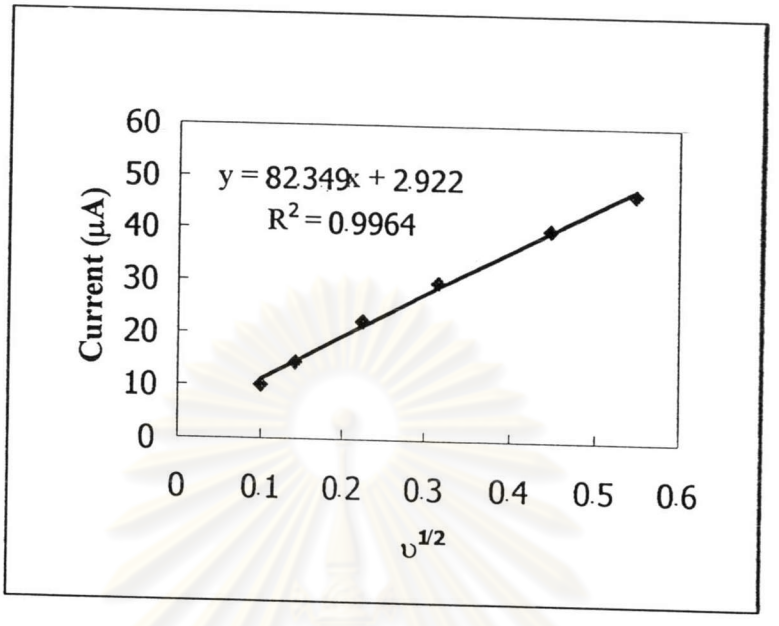

Figure 4.15 The current vs. square root of scan rate ($\upsilon^{1/2}$) curve of 1 mM tetracycline in 0.1 phosphate buffer (pH 2) at Ni-implanted diamond electrode

4.2.5 The analytical performance

Table 4.3 summarizes the analytical figure of merit of tetracycline, chlortetracycline, doxycycline and oxytetracycline at the Ni-implanted diamond electrode by cyclic voltammetry.

4.2.5.1 Tetracycline

Tetracycline was determined using concentrations from 0.005 to 5 mM at the Ni-implanted diamond electrode. From the calibration curve, a good linear response within the concentration range of 0.01-1 mM (Figure 4.16) was obtained with the Ni-implanted diamond electrode. The sensitivity is defined as the slope of calibration plot of tetracycline at the Ni-implanted diamond electrode (38.68 μA/mM). The detection limit (LOD) is defined as the concentration that provides a ratio of current signal to background current noise of at least 3 (S/N≥3). The LOD for

tetracycline using the Ni-implanted diamond electrode was found to be 0.01 mM (10 μM) as shown in Figure 4.17.

Table 4.3 Analytical figure of merit of tetracycline, chlortetracycline, doxycycline and oxytetracycline at the Ni-implanted diamond electrode by cyclic voltammetry.

Analyte	Ni-DIA				
	Linear range (mM)	Sensitivity (μA/mM)	R^2	LOD (mM)	LOQ (mM)
Tetracycline	0.01-1	38.68	0.9979	0.010	0.017
Chlortatrecycline	0.005-0.5	37.28	0.9979	0.005	0.017
Doxycycline	0.005-0.5	38.16	0.9997	0.005	0.017
Oxytetracycline	0.005-0.5	46.02	0.9992	0.005	0.017

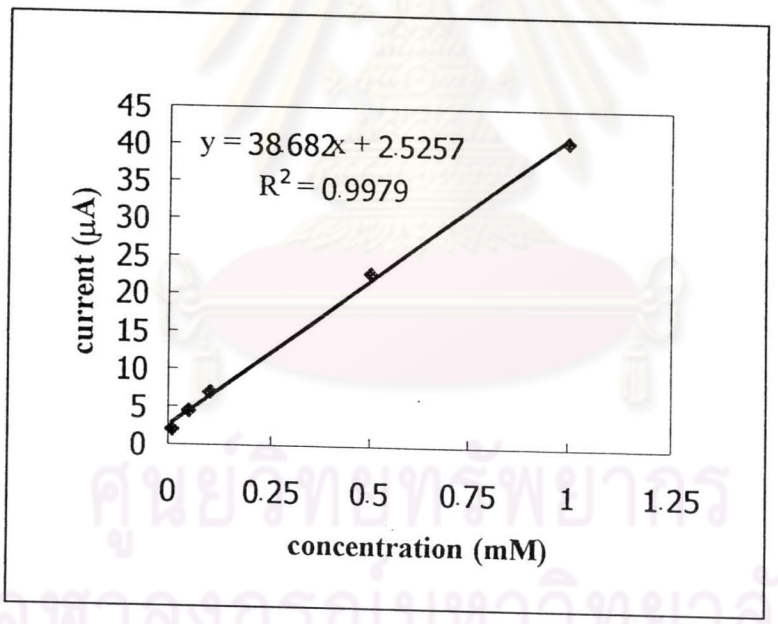

Figure 4.16 Calibration curve of tetraccycline (0.01-1 mM) in 0.1 M phosphate buffer (pH 2) at the Ni-implanted diamond electrode. Tha scan rate was 50 mVs^{-1}

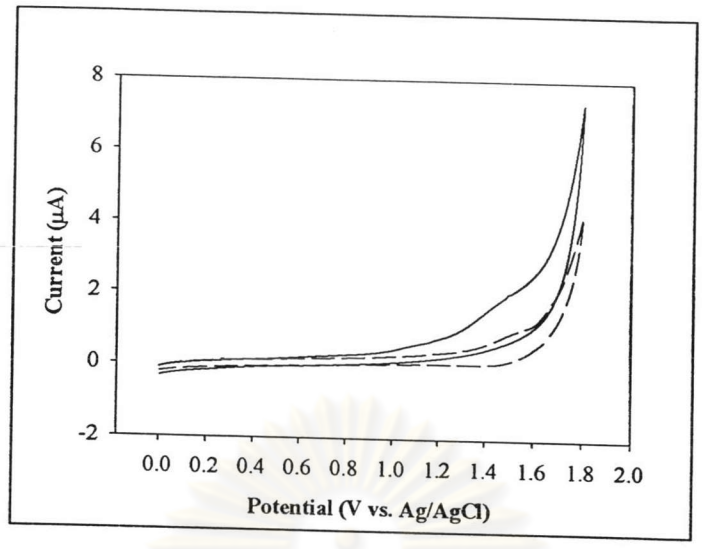

Figure 4.17 Cyclic voltammogram of 0.01 mM tetracycline in 0.1 M phosphate buffer (pH 2) at Ni-implanted diamond electrode (solid line). The scan rate was 50 mVs^{-1}. Background voltammogram is also shown in this Figure (dash line).

4.2.5.2 Chlortetracycline

The oxidation peak current of chlortetracycline solutions at varying concentrations from 0.05 to 5 mM at the Ni-implanted diamond electrode were measured and used to construct calibration curve. From this curve, a good linear response within the concentration range 0.005-0.5 mM (Figure 4.18) was obtained for Ni-implanted diamond electrode. The sensitivity of chlortetracycline at the Ni-implanted diamond electrode (37.28 μA/mM). The LOD for chlortetracycline using the Ni-implanted diamond electrode was found to be 0.005 mM (5 μM) as shown in Figure 4.19.

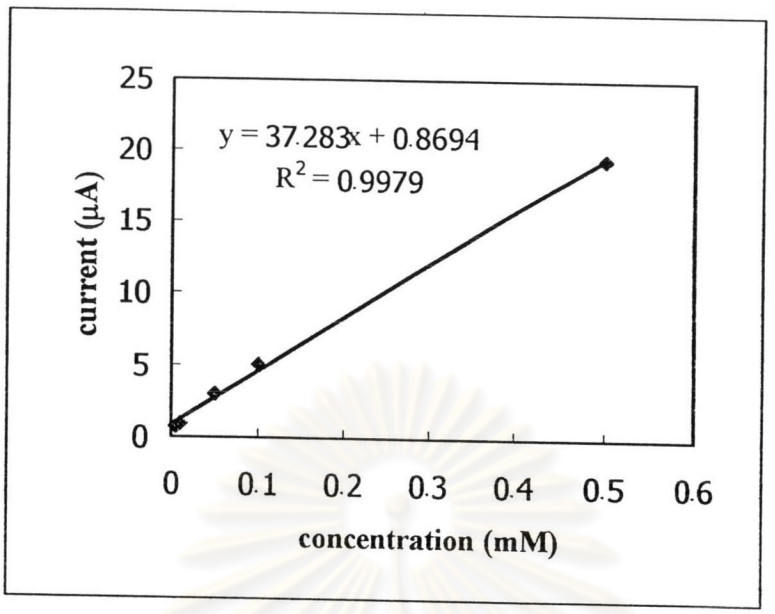

Figure 4.18 Calibration curve of chlortetracycline (0.005-0.5 mM) in 0.1 M phosphate buffer (pH 2) at the Ni-implanted diamond electrode. Tha scan rate was 50 mVs^{-1}

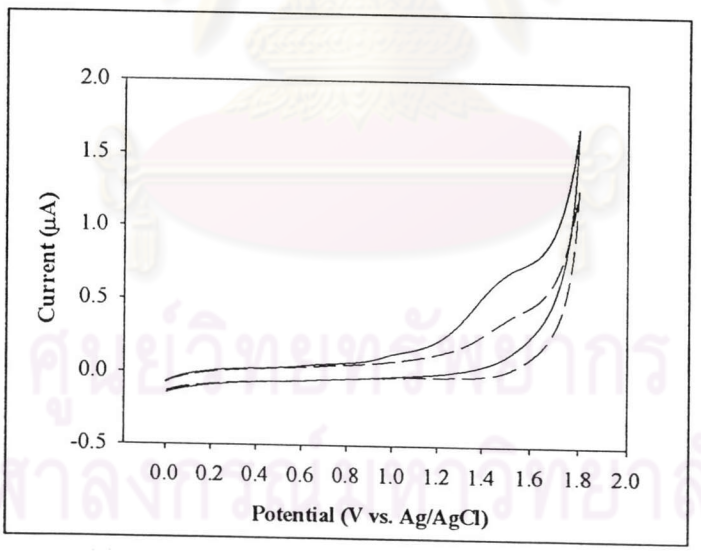

Figure 4.19 Cyclic voltammogram of 0.005 mM chlortetracycline in 0.1 M phosphate buffer (pH 2) at Ni-implanted diamond electrode (solid line). The scan rate was 50 mVs^{-1}. Background voltammogram is also shown in this Figure (dash line).

4.2.5.3 Doxycycline

The oxidation peak current of doxycycline hydrochloride solutions at varying concentration provided the analogous results as described in 4.2.5.2 except that sensitivity was (37.28 μA/mM) and correlation coefficient of 0.9997. The result were also observed with concentration range (Figure 4.20) and detection limit (Figure 4.21)

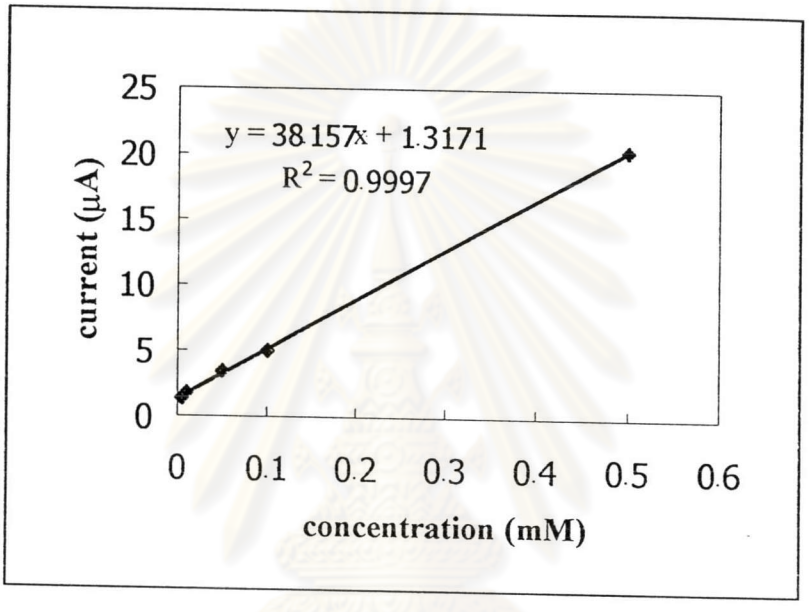

Figure 4.20 Calibration curve of doxycycline (0.005-0.5 mM) in 0.1 M phosphate buffer (pH 2) at the Ni-implanted diamond electrode. Tha scan rate was 50 mVs^{-1}.

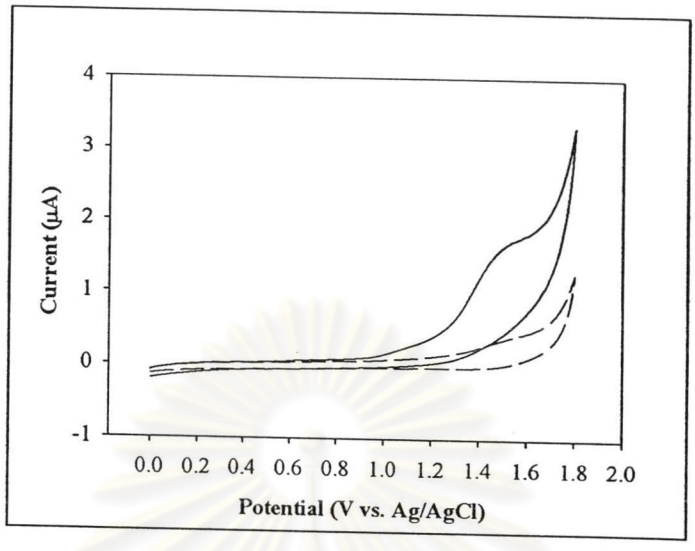

Figure 4.21 Cyclic voltammogram of 0.005 mM doxycycline in 0.1 M phosphate buffer (pH 2) at Ni-implanted diamond electrode (solid line). The scan rate was 50 mVs^{-1}. Background voltammogram is also shown in this Figure (dash line).

4.2.5.4 Oxytetracycline

The oxidation peak current of oxytetracycline hydrochloride solutions at varying concentration provided the analogous results as described in 4.2.5.2 except that sensitivity was (46.2 μA/mM) with a correlation coefficient of 0.9992. The result were also observed with concentration range (Figure 4.22) and detection limit (Figure 4.23)

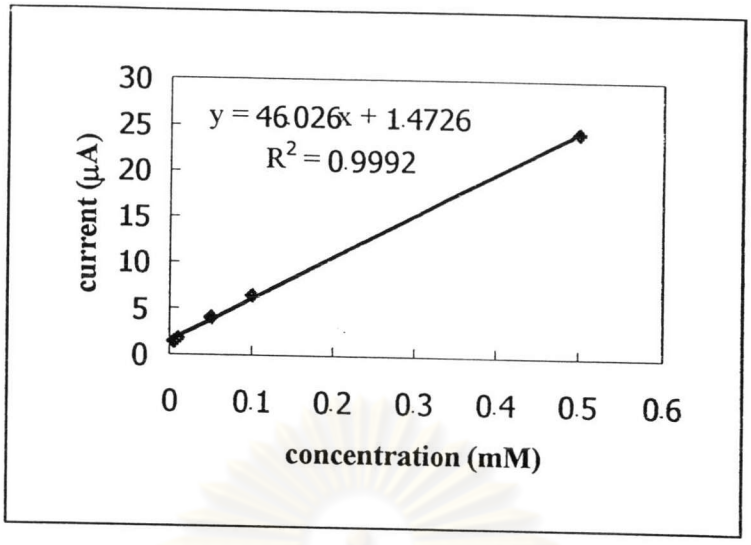

Figure 4.22 Calibration curve of oxytetracycline (0.005-0.5 mM) in 0.1 M phosphate buffer (pH 2) at the Ni-implanted diamond electrode. The scan rate was 50 mVs^{-1}

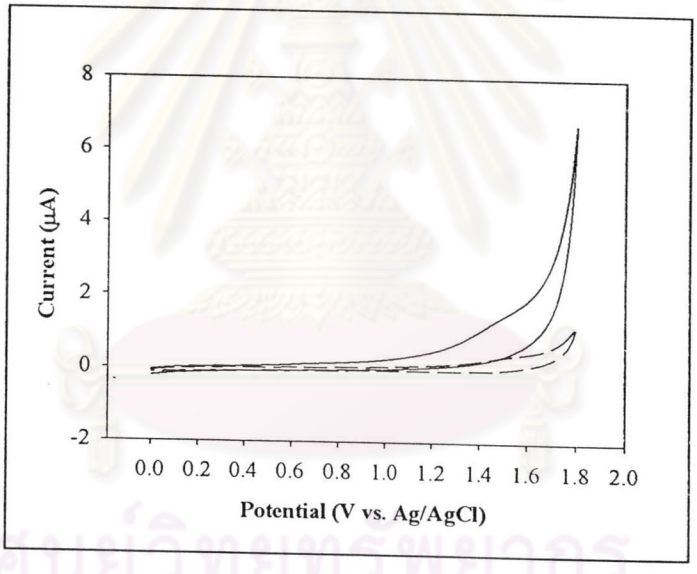

Figure 4.23 Cyclic voltammogram of 0.005 mM oxytetracycline in 0.1 M phosphate buffer (pH 2) at Ni-implanted diamond electrode (solid line). The scan rate was 50 mVs^{-1}. Background voltammogram is also shown in this Figure (dash line).

4.3 Flow injection with amperometric detection

4.3.1 Hydrodynamic voltammetry

This part was carried out in the flow injection system. The variation of potential parameters was obvious from the voltammetric (i-E) response of the analyte. Figure 4.24 shows the hydrodynamic voltammetric i-E curve obtained at the Ni-implanted diamond electrode for 20 µl injection of 100 µM of tetracycline hydrochloride in 0.1 M of phosphate buffer (pH 2) was used as the carrier solution. Each datum represents the average of four injections. The magnitude of the background current at each potential is also shown in this Figure 4.24. The hydrodynamic voltammogram of tetracycline at the Ni-implanted diamond electrode exhibited a well-defined sigmodal shape with a half peak potential at about 1.55 V vs. Ag/AgCl. The half peak that was obtained for tetracycline hydrochloride is near to the peak potential observed in the corresponding cyclic voltammogram at the same concentration. The S/B ratio was calculated from Figure 4.25. The S/B ratio reached a maximum value at a potential of 1.55 V vs. Ag/AgCl as shown in Figure 4.26. Therefore, this potential was fixed for the amperometric potential detection in flow injection analysis experiments.

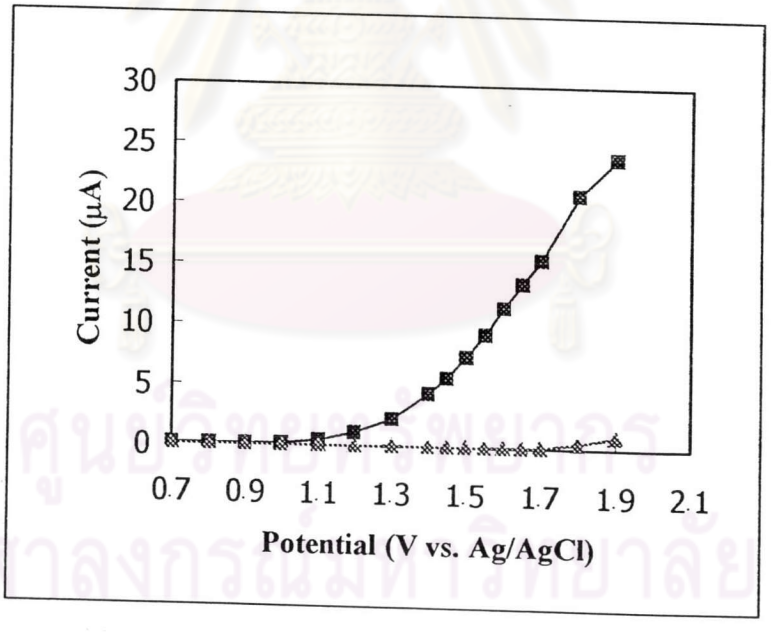

Figure 4.24 Hydrodynamic voltammograms of (-□-) 100 µM of tetracycline in 0.1 M phosphate buffer (pH 2) and (-Δ-) 0.1 M phosphate buffer (pH 2, background current) with four injection of analyte. 0.1 M phosphate buffer (pH 2) was used as a carrier solution, flow rate 1 ml min^{-1}.

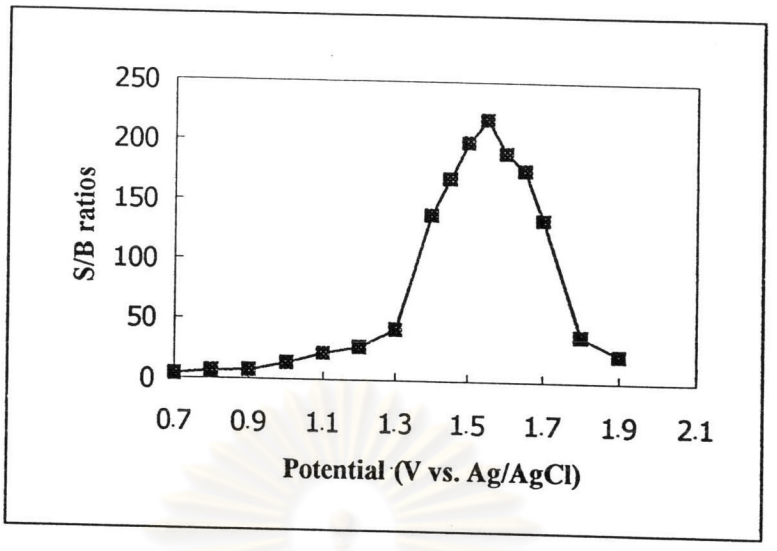

Figure 4.25 Plot of the S/B ratios calculated from Figure 4.34 vs. the applied potential.

After the optimum potential was obtained by hydrodynamic voltammetry, then this potential was used for the amperometric detection. It was also used for the rest of the flow injection experiments for the quantitative analysis of tetracycline hydrochloride.

4.3.2 Calibration and linearity

Calibration curve was obtained with three injections of 20 µl each of analyte solutions in a concentration ranges of 10 nM to 5 mM. The peaks obtained were sharp without tailing. A linear dynamic range was established for over two orders of magnitude. The linear regression equation was obtained by least square adjustment as followed:

$$i = ax + b$$

Where i – current signal (nA),

a – slope or sensitivity (nA/µM),

x – analyte concentration (µM) and b is intercept (nA)

The relation of concentration of tetracycline and peak current is shown in Figure 4.26. The flow injection with amperomatic detection provided a linear dynamic range of 1-100 μM for tetracycline. The sensitivity, this calibration plot is 58.02 nA/μM for tetracycline hydrochloride, with a correlation coefficient of 0.9982. The regression parameters are summerized in Table 4.4.

Table 4.4 Regression statistics for tetracycline hydrochloride

Analytes	Linear dynamic range (mM)	Sensitivity (nA/μM)	Intercept (nA)	R^2
Tetracycline	1-100	58.02	647.6	0.9982

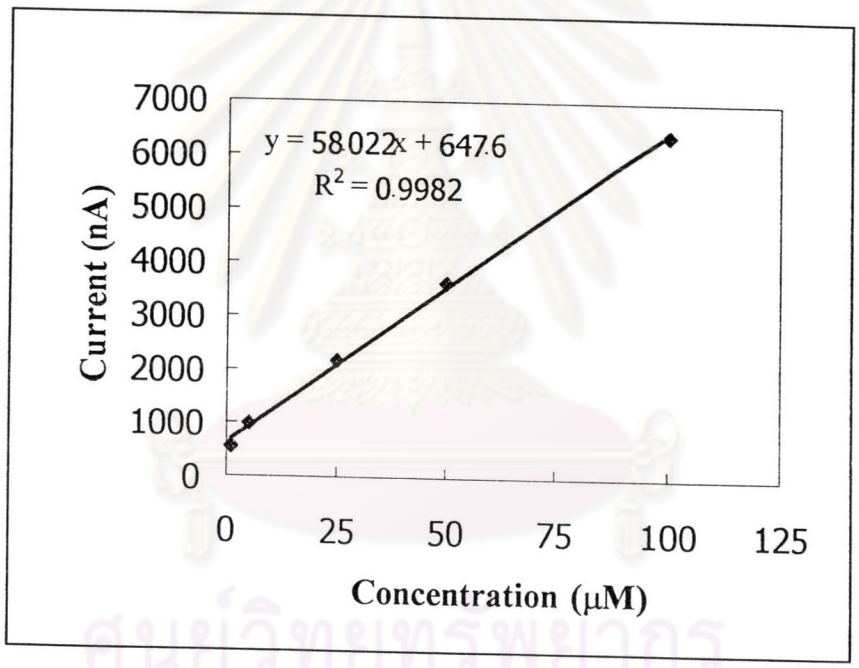

Figure 4.26 Calibration curve (1-100 μM) of tetracycline

4.3.3 Limit of detection (LOD) and Limit of quantitation (LOQ)

LOD and LOQ are defined as the concentration which provides at least three time and ten time of the ratio of the analyte current to noise signal, (S/N ≥ 3) and (S/N≥ 10), respectively. Interestingly, the LOD obtained from this proposed method

was as low as 10 nM for tetracycline hydrochloride. And the LOQ that obtained from this proposed method was 0.03 μM. The LOD of tetracycline at Ni-implanted diamond electrode was 10 nM (Figure 4.27)

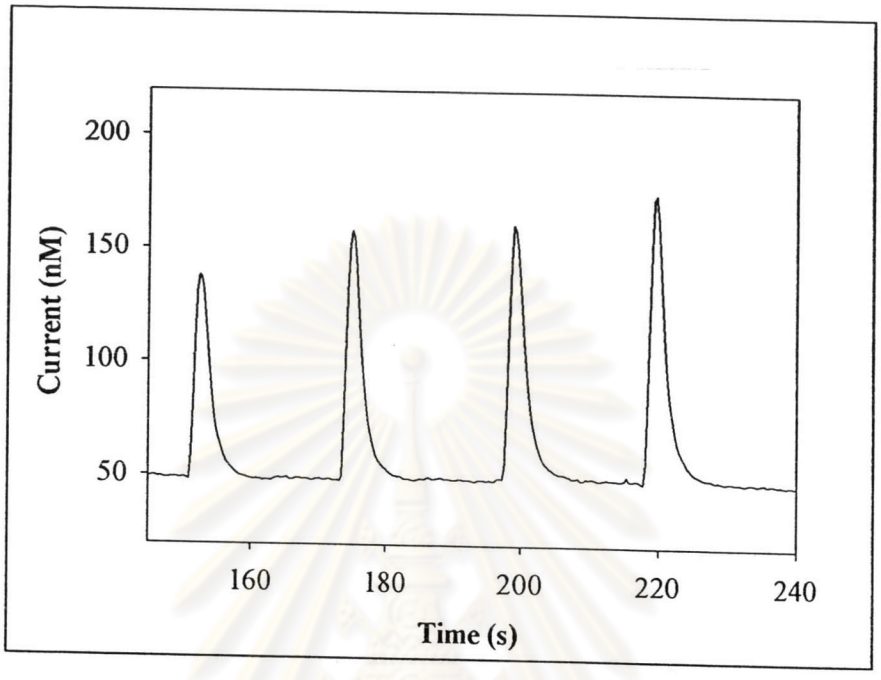

Figure 4.27 Flow injection with amperometric detection results for 10 nM tetracycline in 0.1 M phosphate buffer (pH 2). The flow rate was 1 ml min^{-1}.

4.3.4 Repeatability

The relative standard deviation value was used to reflect the repeatability. Under the optimal potential parameters, 50 μM of the analyte solutions was injected ten times. Figure 4.28 show the flow injection with amperometric detection responses for 50 μM tetracycline. The relative standard deviations was 2.82 %. The peak variability is effected by the past electrochemical history of the Ni-implanted diamond electrode and the manual injection valve of the flow injection system.

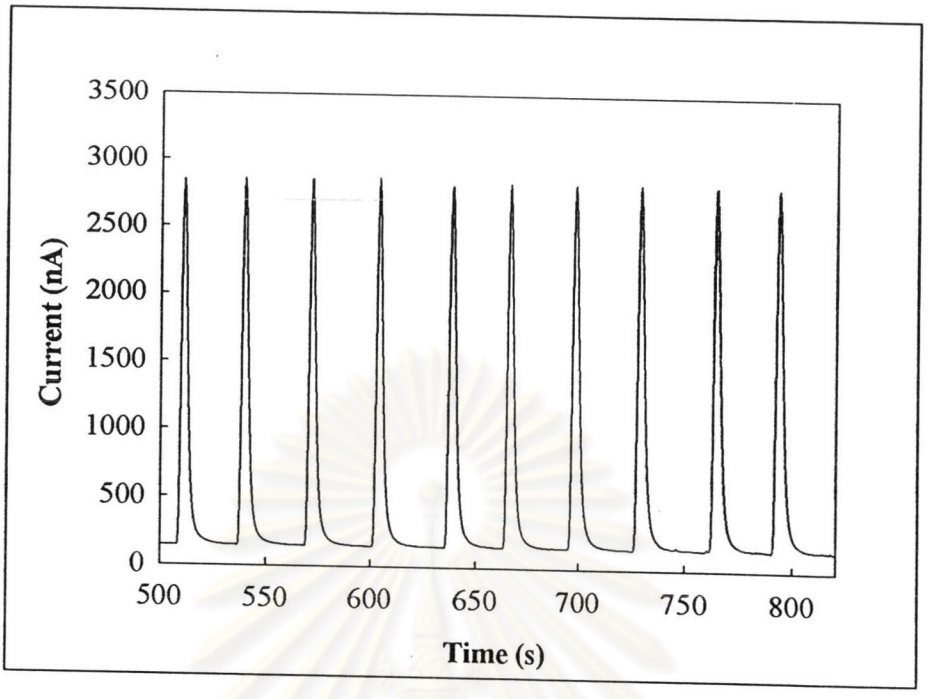

Figure 4.28 Flow injection with pulsed amperometric detection results for 50 μM tetracycline (10 injections) in 0.1 phosphate buffer (pH 2). The flow rate was 1 ml min^{-1}.

4.3.5 Real sample analysis

Flow injection with amperometric detection was applied to the determination of the drug capsules. The standard addition method was used to determine the amount of tetracycline in these samples.

4.3.5.1 Tetracycline

The commercial drug capsule of tetracycline was analyzed by the proposed method. Figure 4.29 shows the standard addition curve of tetracycline capsule. It was found that the slope was 86.16 nA mM^{-1} and the intercept was 1758 nA. The comparison between the labeled amount (250 mg per capsule) and the amount obtained by the suggested method was conducted. Recovery values greater than 97.22 % were found. In order to evaluate this proposed method for the

determination of this compound in drug capsule, the recovery, and within- and between-day studies were carried out on the sample to which the known amounts of tetracycline standards were added. The results of within- and between-day assays are summarized in Table 4.5.

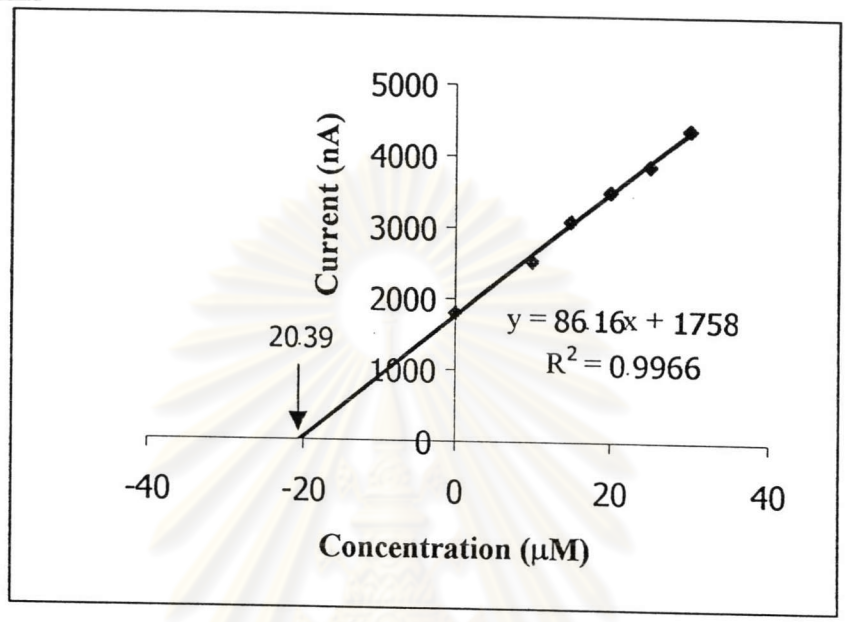

Figure 4.29 Standard addition graph for tetracycline capsule

Table 4.5 Recovery of tetracycline capsule sample with amperometric detection using the Ni-implanted diamond electrode applied to flow injection system of the within- and between-day studies

Amount added ($\mu g\ ml^{-1}$)	Within-day assay		Between-day assay	
	Amount founded ($\mu g\ ml^{-1}$)	Percent recovery (%)	Amount founded ($\mu g\ ml^{-1}$)	Percent recovery (%)
0.36	0.35 ± 0.01	97.22 ± 1.39	0.36 ± 0.01	100.00± 1.97
0.42	0.43 ± 0.00	102.38 ± 0.00	0.41± 0.02	97.61± 3.36
0.48	0.48 ± 0.01	100.00 ± 1.04	0.47± 0.01	97.91± 1.47
0.54	0.54 ± 0.01	100.00 ± 1.85	0.53 ± 0.01	98.14± 1.31
0.60	0.61 ± 0.01	101.66 ± 0.83	0.62 ± 0.01	103.33± 1.17

Recoveries ranging from 97.22-101.66 % and 97.61-103.33 % were obtained for within- and between-day studies, respectively. The results of within- and between-day assays were satisfactory. This proposed method is precise for the determination of tetracycline hydrochloride.

4.4 High performance liquid chromatography

Preliminary separation of tetracycline, chlotetracycline, doxycycline and oxytetracycline were performed on column ODS-3 Inertsil C18 (5 μM, 4.6 x 250 mm i.d.). This column was able to separate tetracycline, chlortetracycline, doxycycline and oxytetracycline under simple isocratic condition of 0.1 M. phosphate buffer (pH 2.5) (A) and 20% acetonitrile (B). Under this condition, all 4 standards were seperated with good resolution within acceptable length of time (27 minutes). Table 3.3 summarized the HPLC condition that will be used throughout this work.

The chromatogram of standard mixture is shown in Figure 4.30.

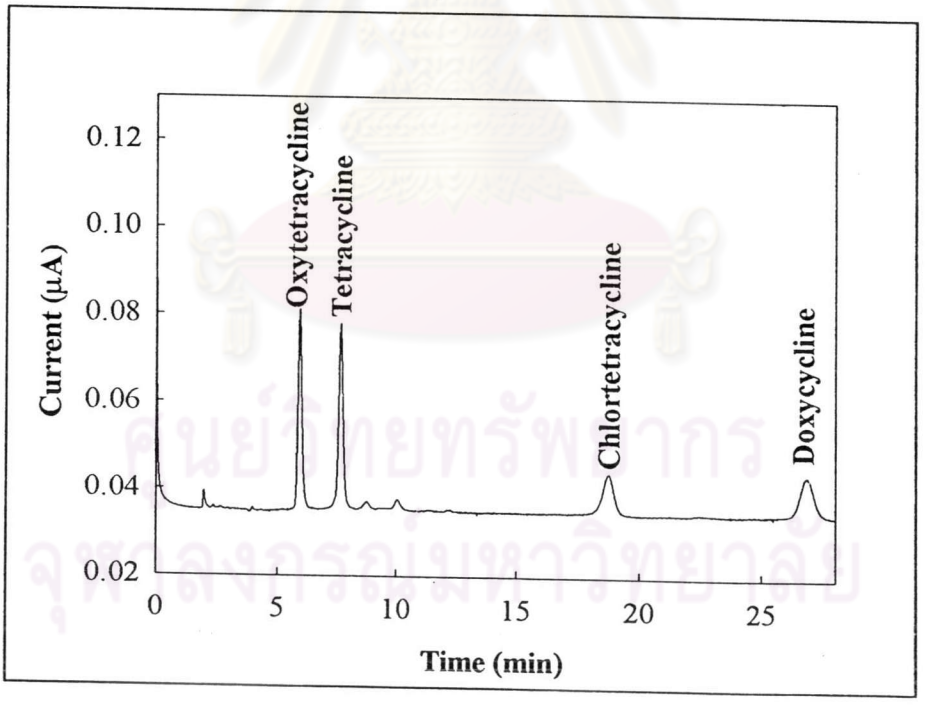

Figure 4.30 Chromatogram of 1 ppm standard mixture seperated on ODS Inertsil C18 column (5 μM 4.6 x 250 mm i.d.) using a mobile phase of phosphate buffer (pH 2.5)- acetonitrile (80:20) with electrochemical detection.

From the chromatogram (Figure 4.30), the orders of elution were oxytetracycline, tetracycline, chlortetracycline and doxycycline respectively. The chromatogram peaks of chlortetracycline and doxycycline are relatively broad because of their affinity to the stationary phase and thus retained in the column longer.

4.4.1 Optimum potential for HPLC

This part was carried out in the HPLC system. Figure 4.31 depicts the optimum potential i-E curve obtained at the Ni-implanted diamond electrode for a 20 µl injection of 100 µM of tetracycline mixture standard solution 0.1 M of phosphate buffer (pH 2.5) was used as the carrier solution. Each datum represents the average of two injections. The magnitude of the background current at each potential is also shown in Figure 4.31. The hydrodynamic voltammogram of tetracycline mixture standard solution at the Ni-implanted diamond electrode exhibited a well-defined sigmodal shape with a half peak potential at about 1.55 V vs. Ag/AgCl. Therefore, this potential was fixed for the amperometric potential detection in HPLC system analysis experiments.

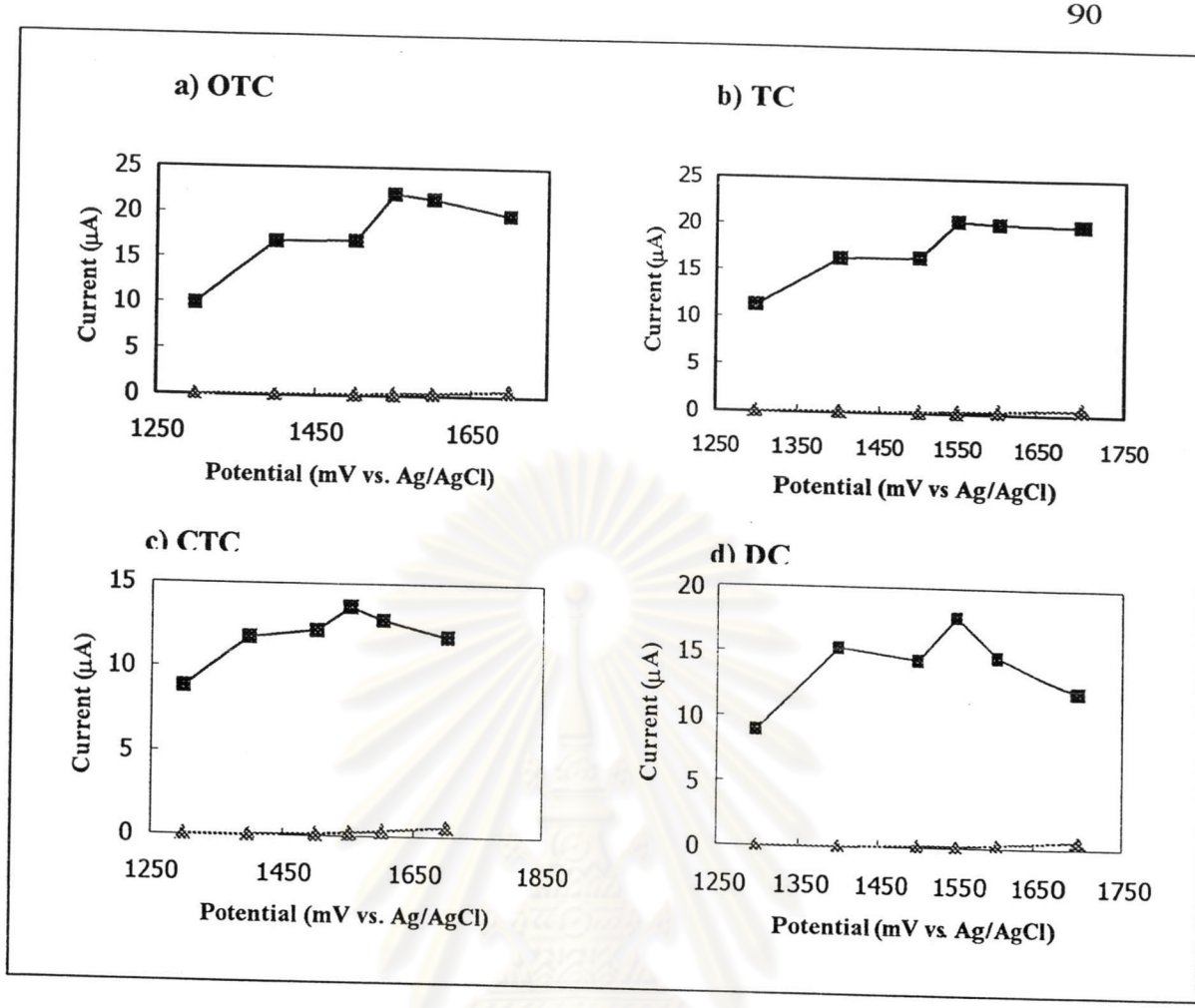

Figure 4.31 Optimum potential of (-□-) 10 ppm of oxytetracycline a), tetracycline b), chlortetracycline c) and doxycycline d) in 0.1 M phosphate buffer (pH 2.5) and (-Δ-) 0.1 M phosphate buffer (pH 2.5, background current) with two injections of analyte. 0.1 M phosphate buffer (pH 2.5) was used as a carrier solution, flow rate 1 ml min^{-1}.

4.4.2 Calibration curve and linear range

The tetracycline mixture standard solutions covering the concentration range of 0.01-100 ppm were analyzed and their peak areas were plotted versus concentration. The regression data are summarized in Table 4.6 Regression plots of the concentration and peak area are shown in Figure 4.32.

From Table 4.6, the data of the 10 point calibration curve was acceptable for quantitation because the correlative coefficient (R^2) obtained were between 0.9975 to 0.9996.

Table 4.6 Linear regression statistics results

Analytes	Linear dynamic range (ppm)	Slope (peak areas units/mg/kg)	Intercept (μA)	R^2
Oxytetracycline	0.05-100	0.0473	0.0562	0.9975
Tetracycline	0.05-100	0.0395	0.0453	0.9977
Chlortetracycline	0.1-100	0.0110	0.0045	0.9990
Doxycycline	0.1-100	0.0111	0.0066	0.9996

The determination of each tetracycline by HPLC can be distinguished by the retention time of 5.97, 7.55, 18.87 and 26.95 min for oxytetracycline hydrochloride, tetracycline, chlortetracycline and doxycycline, respectively.

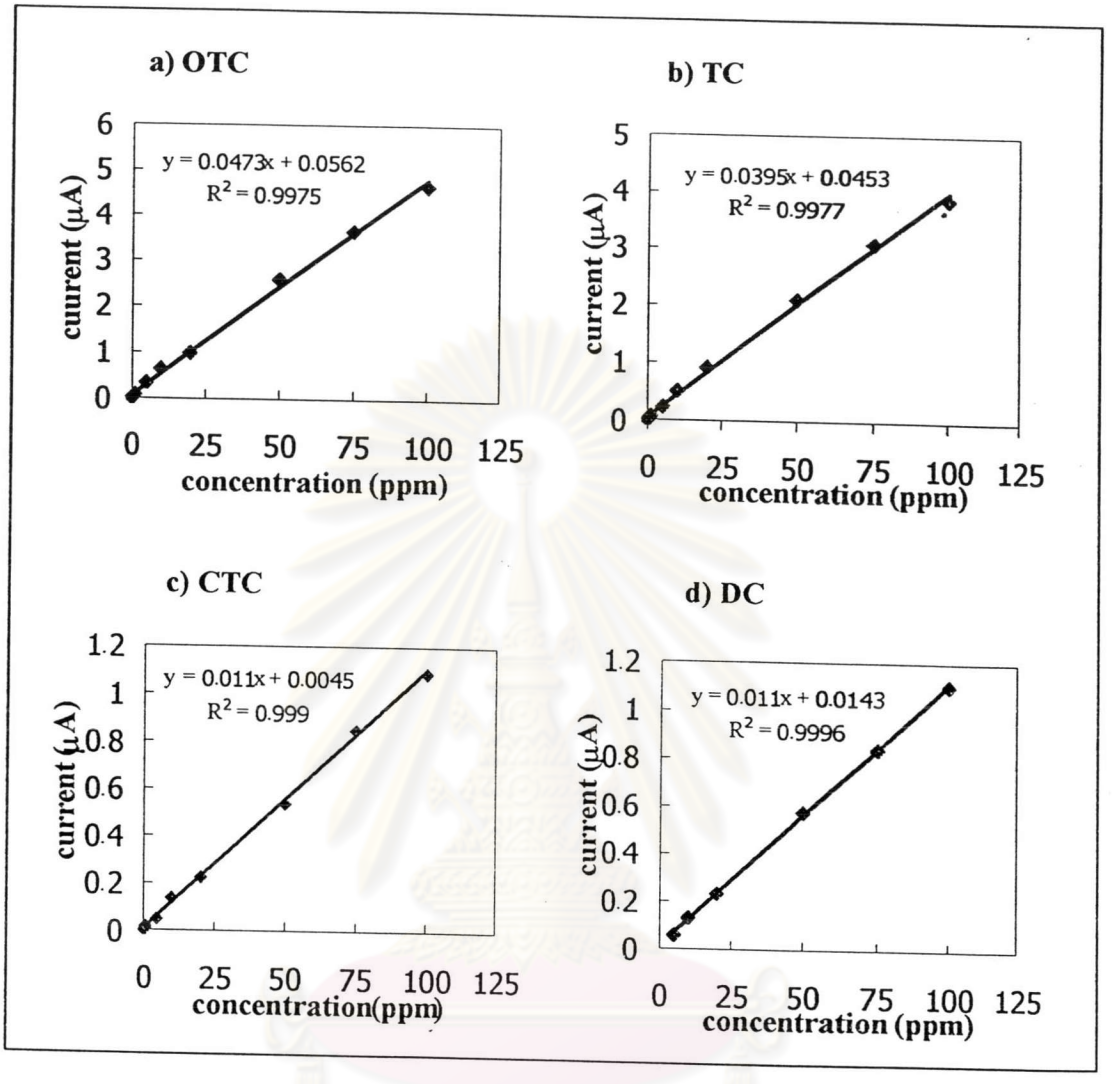

Figure 4.32 Calibration curve of oxytetracycline a), tetracycline b), chlortetracycline c) and doxycycline d) obtained from HPLC data.

4.4.3 Limit of detection (LOD) and Limit of quantitation (LOQ)

The limit of detection (LOD) and limit of quantitation (LOQ) were defined as the concentration of that yielded the peak area of analyte in matrix standard solutions that signalled significantly different from the peak area of noise equal 3 for LOD and 10 for LOQ of each compound. These are shown in Table 4.7.

The limit of detection and limit of quantitation of the 4 tetracyclines are in the range of 0.01-0.05 ppm and 0.03-0.17 ppm respectively.

Table 4.7 The limit of detection and limit of quantitation of analyte in matrix standard solutions.

Analytes	LOD (ppm)	LOQ (ppm)
Oxytetracycline	0.01	0.03
Tetracycline	0.01	0.03
Chlortetracycline	0.05	0.17
Doxycycline	0.05	0.17

4.4.4 Precision

The method for extraction as described in 3.4.6.4 was used to determined %recovery and precision of this method at spiking level of 5 mg/kg for shrimp farming samples and shrimp sea samples.

Table 4.8-4.9 displays the intra-day precision of this method at the spiking level of 5 mg/kg for shrimp farming samples and shrimp sea samples respectively.

Table 4.10-4.11 illustrates the inter-day precision of the method at the spiking level of 5 mg/kg for shrimp farming samples and shrimp sea samples respectively.

Table 4.8 Mean of %Recovery of tetracyclines (intra-day precision) at spiking level of 5 mg/kg in Shrimp farming sample (n=3)

Analytes	%Recovery			Mean±SD	%RSD
	1	2	3		
Oxytetracycline	101.4	100.9	100.8	101.1±0.3	0.3
Tetracycline	101.2	101.6	100.5	100.4±1.7	1.7
Chlortetracycline	100.2	99.4	97.0	98.9±1.6	1.6
Doxycycline	101.8	99.9	101.6	101.1±1.0	1.0

Table 4.9 Mean of %Recovery of tetracyclines (intra-day precision) at spiking level of 5 mg/kg in Shrimp sea sample (n=3)

Analytes	%Recovery			Mean±SD	%RSD
	1	2	3		
Oxytetracycline	107.7	106.4	107.5	107.2±0.7	0.6
Tetracycline	100.9	101.1	101.9	101.3±0.5	0.5
Chlortetracycline	103.0	99.8	98.7	100.5±2.2	2.2
Doxycycline	103.6	99.0	95.9	99.5±3.8	3.8

Table 4.10 Mean of %Recovery of tetracyclines (inter-day precision) at spiking level of 5 mg/kg in Shrimp farming sample (n=6)

Analytes	%Recovery						Mean±SD	%RSD
	1	2	3	4	5	6		
Oxytetracycline	101.5	101.4	100.9	101.4	100.9	100.8	101.1±0.3	0.3
Tetracycline	101.6	100.5	102.8	101.2	101.6	100.5	101.3±0.8	0.8
Chlortetracycline	100.2	99.4	97.0	99.1	98.2	100.4	99.1±1.2	1.2
Doxycycline	97.2	101.8	99.9	101.6	98.9	101.4	100.1±1.8	1.8

Table 4.11 Mean of %Recovery of tetracyclines (inter-day precision) at spiking level of 5 mg/kg in Shrimp sea sample (n=6)

Analytes	%Recovery						Mean±SD	%RSD
	1	2	3	4	5	6		
Oxytetracycline	100.3	102.6	101.1	107.7	106.4	107.5	104.3±3.3	3.1
Tetracycline	101.1	100.0	100.9	100.9	101.7	101.9	101.1±0.6	0.6
Chlortetracycline	102.3	99.6	99.6	103.0	99.8	98.7	100.5±1.7	1.7
Doxycycline	93.7	100.3	94.3	103.6	99.0	95.5	97.7±3.8	3.9

4.4.5 Accuracy

From Table 4.12, %recovery of 4 tetracyclines in Shrimp farming sample at spiking level of 0.5 mg/kg are in the range of 81.6-98.9%, while these of the 1mg/kg, 5 mg/kg and 10 mg/kg spiking levels are in the range of 80.4-99.0%, 87.9-105.0 % and 93.2-109.2%, respectively. And from Table 4.13, %recovery of 4 tetracyclines in Shrimp sea sample at spiking level of 0.5 mg/kg are in the range of 84.2-109.1%, while these of the 1mg/kg, 5 mg/kg and 10 mg/kg spiking levels are in the range of 72.2-97.4%, 80.3-91.7 % and 93.7-109.1%, respectively. These values agree within the acceptable range set forth by AOAC Regulations of %recovery at 75-125 mg/kg level.

Table 4.12 Accuracy of extraction method at spiking level of 0.5, 1, 5 and 10 mg/kg for Shrimp farming sample.(n=3)

Analytes	Mean of %Recovery			
	Spiking level of 0.5 mg/kg	Spiking level of 1 mg/kg	Spiking level of 5 mg/kg	Spiking level of 10 mg/kg
Oxytetracycline	84.8±3.0	96.8±2.7	102.5±3.4	99.6±1.8
Tetracycline	93.3±5.5	85.9±7.7	96.6±2.4	97.0±5.5
Chlortetracycline	91.48±5.3	94.8±5.9	91.6±5.2	97.9±3.8
Doxycycline	89.2±6.7	88.4±3.0	97.7±5.4	103.7±7.4

Table 4.13 Accuracy of extraction method at spiking level of 0.5, 1, 5 and 10 mg/kg for Shrimp sea sample.(n=3)

Analytes	Mean of %Recovery			
	Spiking level of 0.5 mg/kg	Spiking level of 1 mg/kg	Spiking level of 5 mg/kg	Spiking level of 10 mg/kg
Oxytetracycline	94.9±1.6	83.3±4.3	86.8±5.0	96.5±2.4
Tetracycline	92.0±1.1	88.4±4.4	89.2±1.2	96.9±4.6
Chlortetracycline	91.8±8.6	91.9±3.0	86.0±8.0	93.3±5.1
Doxycycline	102.0±9.0	96.2±1.7	90.6±0.1	99.4±2.4

4.4.6 AOAC standard method

- **Standard calibration curve and linear range**

The mixed 3 standard tetracyclines solution covering the concentration range of 0.05-10 ppm were measured. The regression data are summarized in Table 4.14.

From Table 4.14, the data of the 8 point calibration curve is acceptable for quantitation because the correlative coefficient (R^2) obtained were at 0.9975 to 0.9996.

Table 4.14 Linear regression statistics results

Analytes	Linear dynamic range (ppm)	Slope(peak areas units/mg/kg)	Intercept	R^2
Oxytetracycline	0.05-10	46.656	3.9474	0.9996
Tetracycline	0.05-10	55.960	4.3590	0.9995
Chlortetracycline	0.10-10	28.108	1.6850	0.9999

- **Limit of detection (LOD) and limit of quantitation (LOQ)**

The limit of detection (LOD) and limit of quantitation (LOQ) were defined as the concentration of that yielded the peak area of analyte in matrix standard solutions that signalled significantly different from the peak area of noise equal 3 for LOD and 10 for LOQ of each compound. These are shown in Table 4.15

The limit of detection and limit of quantitation of the 3 tetracyclines are in the range of 0.05-0.10 ppm and 0.17-0.33 ppm respectively.

Table 4.15 The limit of detection and of quantitation of analyte in matrix standard solutions

Analytes	LOD (ppm)	LOQ (ppm)
Oxytetracycline	0.05	0.17
Tetracycline	0.05	0.17
Chlortetracycline	0.10	0.33

- **The result of accuracy**

From Table 4.16, %recovery of 3 tetracyclines in Shrimp farming sample at spiking level of 0.5 mg/kg are in the range of 72.5-78.6%, while these of the 1mg/kg, 5 mg/kg and 10 mg/kg spiking levels are in the range of 72.6-80.2%, 77.5-82.5% and 80.2-90.2%, respectively. And from Table 4.17, %recovery of 3 tetracyclines in Shrimp sea sample at spiking level of 0.5 mg/kg are in the range of 74.2-80.2%, while these of the 1mg/kg, 5 mg/kg and 10 mg/kg spiking levels are in the range of 76.2-81.2%, 79.3-85.9% and 90.0-92.5%, respectively. This is within the acceptable range set forth by AOAC Regulations %recovery 75-125.

Table 4.16 Accuracy of extraction method at spiking level of 0.5, 1, 5 and 10 mg/kg for Shrimp farming sample.(n=3)

Analytes	Mean of %Recovery			
	Spiking level of 0.5 mg/kg	Spiking level of 1 mg/kg	Spiking level of 5 mg/kg	Spiking level of 10 mg/kg
Oxytetracycline	78.6±6.5	79.0±6.3	82.5±3.2	89.9±3.8
Tetracycline	75.8±8.2	80.2±5.3	80.0±3.5	90.2±2.1
Chlortetracycline	72.56±5.4	72.6±7.7	77.5±4.2	80.2±4.2

Table 4.17 Accuracy of extraction method at spiking level of 0.5, 1, 5 and 10 mg/kg for Shrimp sea sample.(n=3)

Analytes	Mean of %Recovery			
	Spiking level of 0.5 mg/kg	Spiking level of 1 mg/kg	Spiking level of 5 mg/kg	Spiking level of 10 mg/kg
Oxytetracycline	80.2±5.3	78.4±5.9	85.9±4.5	92.5±3.0
Tetracycline	75.3±7.2	81.2±6.5	82.3±3.7	91.4±2.5
Chlortetracycline	74.2±6.7	76.2±7.0	79.3±4.0	90.0±4.0

Finally results determined tetracyclines in shrimp sample. From Table 4.18-4.19, the comparisons results of 3 methods in 2 shrimp samples at blank sample. The result and chromatograms is shown in APPENDIX.

Table 4.18 Comparisons results of 3 methods in shrimp farming sample

Analyte	Found (mg/kg)		
	HPLC-ECD	AOAC method**	Result for LCFA***
Oxytetracycline	nd*	nd*	nd*
Tetracycline	nd*	nd*	nd*
Chlortetracycline	nd*	nd*	nd*
Doxycycline	nd*	-	-

* Not detected

** AOAC official method 995.09 (Chlortetracycline, Oxytetracycline and Tetracycline in edible animal tissues)

*** Result of Laboratory Center for Food and Agricultural product Co.,Ltd (LCFA)

Table 4.19 Comparisons results of 3 methods in shrimp sea sample

Analyte	Found (mg/kg)		
	HPLC-ECD	AOAC method**	Result for LCFA***
Oxytetracycline	nd*	nd*	nd*
Tetracycline	nd*	nd*	nd*
Chlortetracycline	nd*	nd*	0.07
Doxycycline	nd*	-	-

* Not detected

** AOAC official method 995.09 (Chlortetracycline, Oxytetracycline and Tetracycline in edible animal tissues)

*** Result of Laboratory Center for Food and Agricultural product Co.,Ltd (LCFA)